Effect of Branching on Rod−Coil Block Polyimides as Membrane Materials for Lithium Polymer Batteries

Mary Ann B. Meador,* Valerie A. Cubon,† Daniel A. Scheiman,‡ and William R. Bennett‡

NASA Glenn Research Center, Cleveland, Ohio 44135

Received February 12, 2003. Revised Manuscript Received May 13, 2003

This paper describes a series of rod−coil block copolymers that produce easy-to-fabricate, dimensionally stable films with good ionic conductivity over a range of temperatures for use as electrolytes for lithium polymer batteries. The polymers consist of short, rigid rod polyimide segments alternating with flexible, polyalkylene oxide coil segments. An optimization study was carried out to examine the effects of four variables (degree of branching, formulated molecular weight, polymerization solvent, and lithium salt concentration) on ionic conductivity, glass transition temperature, and dimensional stability in this system.

Introduction

Solid polymer lithium batteries have many advantages over gel systems, including design flexibility, stability with lithium metal, and elimination of complex packaging to contain the liquid phase or provide support.[1] However, poor room-temperature lithium ion conductivity of solid polymer electrolytes continues to limit the utility of such batteries. The poly(ethylene oxide) structure is the basis for many electrolytes currently under study because of its ability to solvate lithium ions. However, long chains of poly(ethylene oxide) tend to crystallize and slow ion mobility at temperatures below about 80 °C. Various approaches to prevent this crystallization are currently under study,[2] including plasticizers,[3] hyperbranched polymers,[4] and use of nanoparticle additives.[5] One of the more intriguing approaches involves use of copolymers that phase-separate into nanodomains. For example, Soo et al.[6] have demonstrated this concept with a system in which one of the domains is a poly(methyl methacrylate) with ethylene oxide side chains and the other is a siloxane. Though both domains consist of polymers that are well above their glass transition temperature (T_g) at room temperature, the interface imparts solid behavior upon films fabricated from the blocks and room-temperature ionic conductivities are quite high.

Recently, block copolymers consisting of short, rigid rod segments alternating with flexible, polyalkylene oxide coil segments have been reported by Okamoto.[7−8] The rod−coil polymers phase-separate into two domains to a high degree, leading to increased selectivity for CO_2/N_2 gas separation. A select group of linear polyurethanes, and polyamide and polyimide oligomers were examined as the rod portion, while the polyether segments were varied from 9 to 201 repeat units long. The copolymers made with linear polyimide rods showed the greatest propensity to phase-separate and the best gas separation properties.

We have synthesized similar rod−coil block co-polyimides, shown in Scheme 1, to examine their behavior as possible electrolytes for lithium polymer batteries.[9] Whereas the coil phase should allow conduction of lithium ions, the more rigid polyimide rod phase, with a very high T_g, should provide even better physical properties at room temperature than that seen for other phase-separated polymer electrolytes.

The coil block used in these polyimides is Jeffamine XTJ-502, a predominantly poly(ethylene oxide) backboned, 2000 molecular weight (about 40 repeat units long) polyether oligomer terminated at each end with amine. The small portion of propylene units also contained in the oligomer should help to reduce the crystallinity in the coil. The rods are made with a central aromatic diamine or aromatic triamine capped on all ends with 3,3′,4,4′-benzophenonetetracarboxilic dianhydride (BTDA) or pyromellittic dianhydride (PMDA). The amine portion of the rods are either *p*-phenylenediamine (PPDA), 3,3′-dimethylbenzidene (DMBZ), or 1,3,5-triaminophenoxy-benzene (TAB). A diamine center produces a linear rod, whereas a triamine center produces a branched rod.

* To whom correspondence should be addressed. E-mail: Maryann.meador@grc.nasa.gov.
† Summer Intern, 2001.
‡ Employed by QSS Group, Inc.

(1) Gray, F. M. *Polymer Electrolytes*; Springer-Verlag: New York, 1997.
(2) Wright, P. V. *MRS Bull.* **2002**, *27*, 597−602.
(3) Kim, Y. T.; Smotkin, E. S. *Solid State Ionics* **2002**, *149*, 29−37.
(4) Nishimoto, A.; Agehara, K.; Furuya, N.; Watanabe, T.; Watanabe, M. *Macromolecules* **1999**, *32*, 1541−1548.
(5) Croce, F.; Persi, L.; Scrosati, B.; Serraino-Fiory, F.; Plichta, E.; Hendrickson, M. A. *Electrochim. Acta* **2001**, *46*, 2457.
(6) Soo, P. P.; Huang, B.; Sadoway, D. R.; Mayes, A. M. *J. Electrochem. Soc.* **1999**, *146*, 32.
(7) Yoshino, M.; Ito, K.; Kita, H.; Okamoto, K. *J. Polym. Sci: B Polym. Phys.* **2000**, *38*, 1707−1715.
(8) Okamoto, K.; Fujii, M.; Okamyo, S.; Suzuki, H.; Tanaka, K.; Kita, H. *Macromolecules* **1995**, *28*, 6950−6958.
(9) Initial screening of other rod and coil combinations was reported in Meador, M. A. B.; Cubon, V. A.; Schieman, D. A.; Bennett, W. *11th International Meeting on Lithium Batteries*, June 23−28, 2002, *Meeting Abstracts*, 153; The Electrochemical Society: Pennington, NJ.

10.1021/cm0301726 CCC: $25.00
Published on Web 06/20/2003

Scheme 1. Synthesis of Rod−Coil Polyimide Copolymers

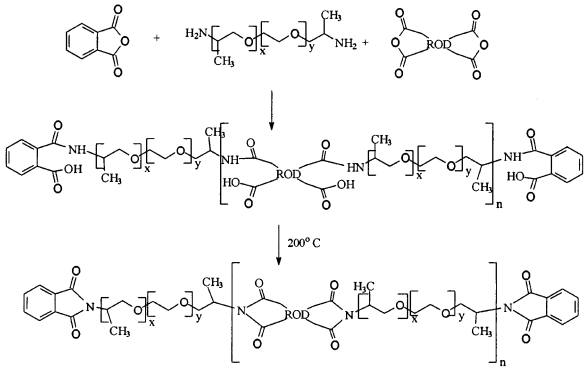

Rods

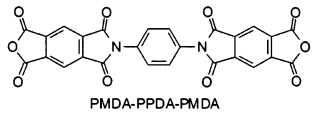

PMDA-PPDA-PMDA

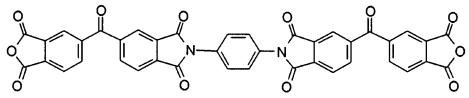

BTDA-PPDA-BTDA

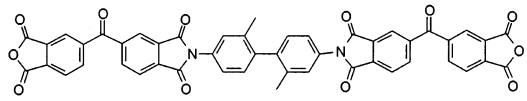

BTDA-DMBZ-BTDA

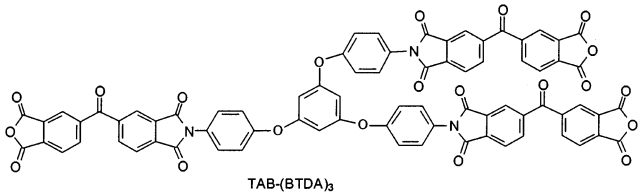

TAB-(BTDA)$_3$

Coil

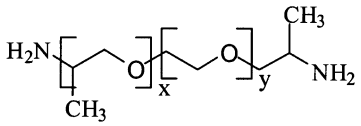

Jeffamine XTJ-502
MW=2000, x=5, y=39.5

Herein, we describe an optimization study of lithium ion conductivity in these polymers. The study was carried out by examining the effect of several parameters (degree of branching and number of repeat units in the polymer) on ionic conductivity and dimensional stability in this system. In all cases, phthalic anhydride (PA) was used to control the molecular weight of the polymer. The molecular weight was formulated to be between 6000 and 60 000 g/mol, corresponding to a number of repeat units, *n*, ranging from about 1.4 to 10.8. We also examined the effect of the concentration of lithium ions, using lithium trifluoromethane sulfonamide as salt. Statistically designed experiments were used to examine the effects of these variables and interactions among variables on the ionic conductivity and physical properties of the each of the films produced.

Experimental Section

General. All reagents were handled in an MBraun glovebox with attached vacuum oven under an argon atmosphere maintained at <1 ppm H_2O. Diamine-capped polyalkyleneoxide oligomer, XTJ-502 (2000 molecular weight) was obtained from Huntsman Corporation. 3,3′,4,4′-benzophenonetetracarboxilic dianhydride (BTDA), pyromellittic dianhydride (PMDA), *p*-phenylenediamine (PPDA), and phthalic anhydride (PA) were obtained from Aldrich Chemical Co. 1,3,5-triaminophenoxy-benzene (TAB) was obtained from Triton Systems. All of these monomers were used as received without further purification. Tetrahydrofuran (THF) and *N*-methylpyrrolidinone (NMP) used as solvents were obtained from Fisher and dried before use. Acetonitrile solvent (Baker HPLC grade) was used as-received.

Lithium trifluoromethane sulfonimide ($LiN(CF_3SO_2)_2$) was purchased from 3M. The salt was vacuum-dried for 24 h at 115 °C before being transferred to the glovebox. Poly(ethylene) oxide (M_v = 500 000) was purchased from Aldrich and used as received.

Ionic Conductivity. Ionic conductivity was measured by electrochemical impedance techniques, using a Solartron/Schlumberger model 1250 FRA and model 1286 Electrochemical Interface. Samples of cured polymer electrolyte were cut from the parent sheet and carefully measured to determine thickness and area. Samples were mounted in a symmetric cell between 304 stainless steel blocking electrodes. Polyester shim material was used to maintain material thickness during the test and to keep the polymer sample from flowing at elevated temperature. Conductivity was measured over the range of 0 to 80 °C.

Polymers were also characterized by differential scanning calorimetry (DSC) from −90 to 300 °C using a Q1000 calorimeter manufactured by TA Instruments. Thermal gravimetric analysis (TGA) was obtained using a TA Instruments high-resolution TGA2950 analyzer. Fourier transform infrared spectroscopy (FT-IR) was obtained from KBr pellets using a Nicolet 5100 spectrometer. Gel permeation chromatography (GPC) was done using a Waters 6000K pump and a differential refractive index detector (R401) in THF using four Waters Ultra-Styragel columns in series (10^4, 10^3, 500, and 100) giving an effective range of separation of 600 K to 50 g/mol. Polystyrenes were used as reference standards.

Nuclear magnetic resonance spectroscopy (NMR) was carried out on a Bruker Avance 300 spectrometer using a high-resolution magic angle spinning (HRMAS) probe at a spinning rate of 4.5 kHz. Polymer samples were swelled with $CDCl_3$ which was also used as an internal reference. A Shore Type-A hardness tester (BYK Gardener) was modified and applied to measure the depth of penetration for all the films.

Experimental design and analysis was carried out using RS/Series for Windows, including RS/1 version 6.01, and RS/Discover and RS/Explore Release 4.1, available from Domain Manufacturing Corporation.

Preparation of Polymers. The polymers were prepared in the glovebox under an argon atmosphere at <1 ppm water. Drying and final cure were carried out in a vacuum oven connected directly to the glovebox. The polymers were synthesized in 20-g batches, following the same procedure throughout. For the sake of brevity, some illustrative examples follow.

Fully Branched Polyimide−Polyether with a Formulated Molecular Weight of 60 000, *n* = 10.72 g/mol (run 27). Jeffamine XTJ-502 coil (14.95, 7.5 mmol), BTDA (3.45 g, 10.7 mmol), and PA (0.63 g, 4.25 mmol) were combined in 20 mL of dry ***N***-methylpyrrolidinone and stirred overnight to dissolve. TAB (1.43 g, 3.57 mmol) and 10−15 mL NMP were added and stirring was continued for approximately 4 h until the entire solid was dissolved. The resulting yellow polyamic acid solution was 27.6% solids by weight. Enough of the solution to give a 2-g film (7.255 g of solution) was cast into a

2-in.-diam aluminum boat. The solvent was removed by heating the boat in a vacuum oven connected to the drybox at 70 °C for 24 h, followed by 100 °C for 12 h. Curing in the vacuum oven at 200 °C resulted in a yellow rubbery film. HR-MAS NMR: 13C δ 14.12, 16.36, 45.93, 46.48, 69.66, 72.34, 74.22, 113.9, 118.95, 122.17, 122.77, 123.09, 127.21, 131.52, 133.11, 134.60, 140.59, 154.85, 166.23, 167.36, 192.15. DSC: T_g −55.56 °C, endotherm 18.5 °C. FT-IR (cm^{-1}): 2869.9, 1713.1, 1377.7, 1099.7.

Lithium trifluoromethane sulfonimide (0.72 g) was dissolved in enough of the 27.6% solid polyamic acid solution to give 3 g of polymer (10.87 g). This gives a 13:1 ratio of polyether oxygens to lithium ion in solution. The polymer−salt solutions were cast onto stainless steel boats and submitted to a drying and curing procedure the same as that used for the neat films. The resulting salt-containing films were cut into two parts—one for conductivity measurement, the other for thermal analysis and FT-IR—and were sealed in argon until testing.

DSC: T_g = −45.5 °C. FT-IR (cm^{-1}): 2878.4, 1714.1, 1351.7, 1190.6, 1097.3.

Linear Polyimide Polyether with Formulated Molecular Weight of 10 000 g/mol, n = 2.89 (run 16). Jeffamine XTJ-502 coil (15.55, 7.8 mmol), BTDA (3.72 g, 11.5 mmol), and PA (0.59 g, 3.98 mmol) were combined in 20 mL of dry tetrahydrofuran (THF) and stirred overnight to dissolve. PPDA (0.62 g, 5.73 mmol) and 25−30 mL of THF were added and stirring was continued for approximately 4 h until the entire solid was dissolved. The resulting yellow polyamic acid solution was 23.3% solids by weight. Enough of the solution to give a 2-g film (8.57 g of solution) was cast into a 2-in.-diam aluminum boat. The solvent was removed by gentle heating on a hot plate overnight. Curing in the vacuum oven attached to the drybox at 200 °C resulted in a yellow-orange, insoluble film. HR-MAS NMR ($CDCl_3$): ^{13}C δ 13.97, 16.23, 45.60, 46.34, 68.20, 69.51, 72.18, 74.04, 122.00, 122.65, 122.92, 130.94, 131.36, 132.99, 134.21, 134.51, 140.46, 166.05, 167.18, 191.97. DSC: T_g = −47.0 °C, endotherm 23.8 °C. FT-IR (cm^{-1}): 2869.4, 1713.1, 1380.5, 1097.6.

Lithium trifluoromethane sulfonimide (0.374 g) was dissolved in enough of the 23.3% solid polyamic acid solution to give 3 g of polymer (10.87 g). This gives a 40:1 ratio of polyether oxygens to lithium ion in solution. The polymer−salt solution was cast onto stainless steel boats and submitted to a drying and curing procedure the same as that used for the neat films. The resulting salt-containing films were cut into two parts—one for conductivity measurement, the other for thermal analysis and FT-IR—and were sealed in argon until testing. HR-MAS NMR: (CDCL3) ^{13}C δ 13.94, 16.06, 46.35, 69.30, 72.03, 73.94, 118.94, (q, j = 321 Hz, salt), 122.15, 122.73, 125.34, 131.42, 133.26, 134.25, 134.66, 140.54, 166.17, 192.26.

DSC: T_g = −48.9 °C. FT-IR (cm^{-1}): 2872.1, 1714.0, 1381.8, 1352.4, 1192.1, 1097.2.

Poly(ethylene oxide) Film. Stock solutions of poly(ethylene oxide) and lithium imide salt were prepared in acetonitrile (3 wt % and 21 wt %, respectively). Solutions were mixed together at room temperature in predetermined amounts by magnetic stirring for approximately 48 h.

Polymer electrolyte films were prepared by casting. The polymer/salt solution was transferred to a Teflon Petri dish and vacuum de-gassed to disengage bubbles. The acetonitrile was allowed to evaporate for 48 h at glovebox temperature, ~25 °C. The dried films were further cured overnight at 40 °C under vacuum. This process produced flexible, 90-μm-thick films with a 16:1 EO/Li salt content. DSC: T_g = −40.8 °C, T_m = 50.3 °C. FT-IR (cm^{-1}): 2886.5, 1467.0, 1353.8, 1341.8, 1192.5, 1098.0.

Results and Discussion

Initially, a screening study was carried out to examine the effects of different aromatic dianhydrides, diamines, or triamines on ionic conductivity of the rod−coil hybrid films. In this initial phase, polymers made up of PPDA with PMDA, PPDA with BTDA, DMBZ with BTDA, and TAB with BTDA, and the 2000 molecular weight Jeffamine were synthesized with a formulated molecular weight of 10 000 or 30 000 g/mol, as described. The first three formulations represent increasing lengths of rod and the last introduces branching to the structure. All films were fabricated from NMP using oxygen-to-lithium ratios of 20:1. Ionic conductivity measured by electrochemical impedance is shown in Figure 1 for a sampling of the films. From this graph, it is immediately evident that films produced with PMDA had considerably lower conductivity. It was thought that these short, very stiff rods would profoundly affect phase separation and hence raise conductivity. This proved not to be the case. Likewise, there appears to be no advantage to using the longest rods containing DMBZ, as films made from this diamine had lower conductivity than comparable formulations with PPDA.

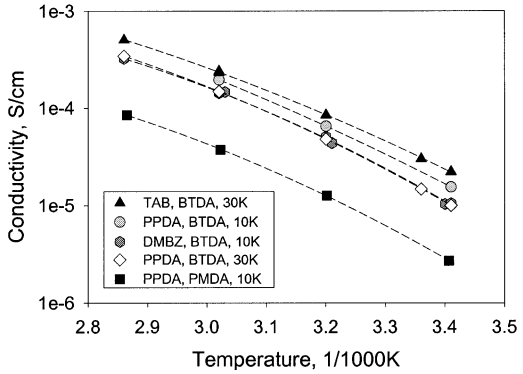

Figure 1. Comparison of ionic conductivities of a variety of rod−coil polymers.

Scheme 2. Structure of Rod−Coil Polymer

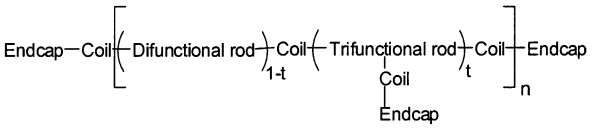

The highest ionic conductivities from the initial screening were obtained using TAB or PPDA with BTDA. We wished to explore polymers containing these monomers in more detail to gain insight into how to improve the conductivity. It was thought that four variables—degree of branching, number of repeat units, salt concentration, and polymerization solvent—used in formulating and synthesizing the polymer films could affect the ionic conductivity and other properties of the rod−coil polymers. The degree of branching through the use of triamine (TAB) versus diamine (PPDA) in the polyimide rods would effectively increase the number of coils not constrained at both ends by the polymer chain. In the linear polymer, coils within the polymer chain would be constrained on two ends while the coils attached to the terminal ends would be unconstrained on one side. In the fully branched polymer, a side chain coil would be attached to each trifunctional rod, giving one mobile coil per every repeat unit plus the chain ends. As shown in Scheme 2, t is the fraction of triamine used in place of diamine and, hence, the fraction of trifunctional rods.

The number of repeat units, n, in the polymer may also affect properties. Larger n should result in a more robust, mechanically resilient film, whereas smaller n

may result in higher mobility and therefore higher ionic conductivity. Salt concentration, *s*, affects the number of lithium ions available for transport. The values used are based on the ratio of lithium and oxygen atoms in the coils only, as it is anticipated that the oxygen in the polyimide rods would have a negligible role in solvating the lithium ions. Polymerization solvent, *p*, was also evaluated as a variable. NMP is typically used for polyimide synthesis because the polyamic acids are not often soluble in other lower boiling solvents. However, the addition of the polyalkyl ether coil unit does allow most of the polyamic acids to be soluble in THF. The lithium salt, on the other hand, is more soluble in THF. Therefore, the solvent could influence the final properties of the polymers.

We used a statistical experimental design approach to evaluate the effects of these four variables on the polymer properties or responses. We wished to entertain a full quadratic model of the form

$$\text{Response} = A + Bt + Cn + Ds + Ep + Ft^2 + Gn^2 + Hs^2 + Itn + Jts + Ktp + Lns + Mnp + Nsp$$

where *A* through *N* are coefficients empirically derived from experimental data. The model contains terms for first-order effects of all four variables and second-order terms for *t*, *n*, and *s*, as well as all two-way interaction terms. To evaluate first and second-order effects of *t*, *n*, and *s*, a minimum of three levels of each variable must be considered. The three levels of *t* used are 0% TAB/100% PPDA, 50% TAB /50% PPDA, and 100% TAB/0% PPDA. Three levels of *s*, based on the ratio of lithium ion to ether oxygen in the polymer (0.025, 0.05, and 0.075, corresponding to 40:1, 20:1, and 13:1 oxygen-to-lithium ratio, respectively) were also studied. In addition, *n* was evaluated from 1.4 to 10.7 repeat units, corresponding to a formulated molecular weight of 6000 to 60 000 g/mol. Two levels of the discrete variable *p*, NMP and THF, were used to make the polymers.

A full-factorial design to evaluate this model would contain 54 experiments. To minimize the number of experiments in the study, we used a *d*-optimal experimental design strategy.[10] In this type of nonclassical design, a set of runs is computer-generated from the 54 candidate runs to evaluate the desired model most efficiently. The scope of the design can be described as a box (shown in Figure 2) with each of the three axes representing three continuous variables (*n*, *s*, and *t*). The symbols in the box represent each of the runs. Runs in the design synthesized in NMP are shown as shaded squares, and those in THF are shown as open circles. The total number of unique experiments in the *d*-optimal design is 23. In addition, 4 runs from across the design are repeated to assess model reliability and accuracy, assuming error is consistent across the whole design.

(10) Initially, we started with a more classic design, using formulated molecular weight as a variable rather than the number of repeat units, *n*. It quickly became clear on analysis of data after most of the runs were complete that models could not be derived on the basis of formulated molecular weight. After much reexamination of the data, it was determined that *n* provided a more rational fit, meaning for the responses studied, linear polymers at 30 000 g/mol ($n = 10.35$) are more comparable to branched polymers at 60 000 g/mol ($n = 10.72$). Likewise, branched polymers at 10 000 g/mol ($n = 1.44$) are more comparable to those at 6000 g/mol ($n = 1.4$) linear polymers. These extreme runs were added to the design, necessitating the use of *d*-optimal methodology.

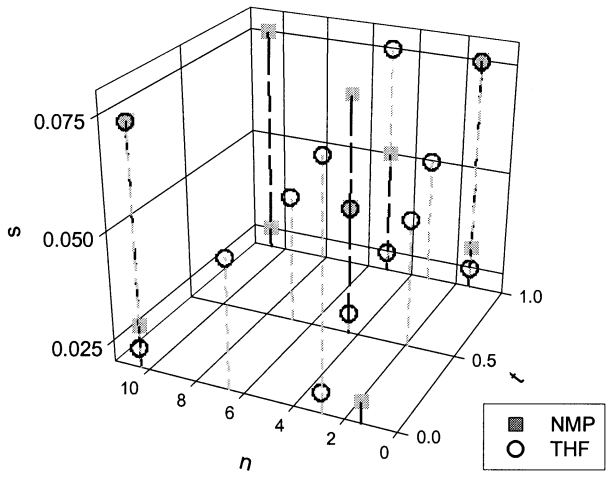

Figure 2. Plot of runs carried out in the *d*-optimal experimental design.

The 27 runs in the experimental design study were carried out in the randomized order shown in Table 1. The resulting data are also summarized in Table 1, including T_g with and without the inclusion of lithium salt, T_m, and ionic conductivity.

The polymers were synthesized as described by stirring the BTDA, end cap, and the Jeffamine polyether until dissolved, followed by addition of aromatic diamine or triamine to achieve highly viscous polyamic acid solutions. Order of addition of the monomers proved to be important, especially for the formulations containing TAB. Mixing the TAB and BTDA together, followed by addition of Jeffamine resulted in insoluble gels, presumably from formation of hyperbranched polyamic acid structures.

Imidization was carried out in a vacuum oven at 200 °C. Because the resulting rubbery polyimide films are all insoluble after final cure, gel permeation chromatography (GPC) was carried out on the polyamic acid solutions in THF. GPC data were analyzed by multiple linear least-squares regression. A mathematical model describing the molecular weight (M_w) in terms of the *n* value and percent triamine was derived. All independent variables were transformed to the −1 to 1 range prior to modeling to minimize correlation among terms. M_w was normalized using a log transform. Terms not statistically significant (<90% confidence) were dropped from the model one at a time by the stepwise modeling technique. Significant terms in the model (all >96% confidence) included a first-order effect of triamine concentration, as well as first and second-order effects of *n* value.

A response surface for M_w is shown in Figure 3. Predicted M_w from the model ranged from 5700 to 41 000 g/mol for polyamic acid over the range of the data, compared to 6000 to 60 000 g/mol for the formulated molecular weight. In addition to the fact that polyamic acid is susceptible to hydrolysis in air, a drop-off of M_w in the high-molecular-weight range is not unexpected, considering the highly branched polymers would present a smaller hydrodynamic radius compared to those of polystyrene standards. Standard error of regression of the model for log M_w was 0.077 with $r^2 = 0.81$.

Thermogravimetric analysis (TGA) and TGA-FTIR were used to monitor residual solvent for all films.

Table 1. Data from Experimental Design Study

run	FMW g/mol	*n*	triamine %	salt conc.	solvent	Log cond, RT, S/cm	T_g, °C w/Li salt	T_g, °C, neat	T_m, °C, neat	penetration depth, %
1	20000	4.40	0.5	0.05	THF	−4.96	−43.3	−50.9	26.68	54
2	20000	4.40	0.5	0.075	THF	−5.20	−38.2	−50.3	26.10	45
3	10000	2.89	0	0.075	THF	−5.05	−37.9	−53.5	23.23	61
4	20000	4.40	0.5	0.025	THF	−5.31	−48.7	−49.9	23.83	38
5	20000	3.29	1	0.05	THF	−4.97	−42.3	−49.0	28.12	42
6	20000	4.40	0.5	0.05	THF	−4.98	−41.4	−50.3	26.35	39
7	20000	6.62	0	0.05	THF	−5.11	−42.9	−53.0	22.05	49
8	30000	10.35	0	0.075	THF	−5.20	−36.4	−51.7	21.76	52
9	30000	5.15	1	0.025	THF	−5.05	−47.8	−50.5	27.04	45
10	10000	1.92	0.5	0.05	THF	−5.03	−44.4	−52.0	27.67	63
11	20000	4.40	0.5	0.05	THF	−5.11	−42.8	−47.3	24.45	48
12	10000	1.44	1	0.075	THF	−5.08	−37.3	−47.6	29.39	55
13	10000	1.44	1	0.025	THF	−4.98	−48.4	−47.4	26.54	58
14	30000	5.15	1	0.075	THF	−5.11	−37.6	−49.3	26.42	36
15	20000	4.40	0.5	0.05	THF	−5.25	−42.4	−51.3	24.08	52
16	10000	2.89	0	0.025	THF	−5.04	−48.9	−49.3	23.76	52
17	30000	10.35	0	0.025	THF	−5.07	−47.6	−50.3	18.69	37
18	10000	1.44	1	0.03	NMP	−5.04	−45.5	−51.9	25.29	63
19	10000	1.44	1	0.075	NMP	−5.17	−37.2	−52.0	25.07	71
20	30000	10.35	0	0.03	NMP	−5.04	−45.9	−54.2	22.04	34
21	30000	10.35	0	0.075	NMP	−5.22	−36.4	−53.9	21.65	52
22	10000	2.89	0	0.05	NMP	−4.91	−45.4	−52.8	19.97	45
23	30000	5.15	1	0.05	NMP	−4.91	−45.4	−50.3	20.07	52
24	10000	1.44	1	0.075	THF	−5.06	−38.5	−52.8	21.84	54
25	60000	10.72	1	0.025	NMP	−4.72	−53.7	−55.9	16.85	42
26	6000	1.40	0	0.025	NMP	−4.67	−53.1	−59.1	21.33	86
27	60000	10.72	1	0.075	NMP	−4.75	−45.5	−55.6	18.51	54

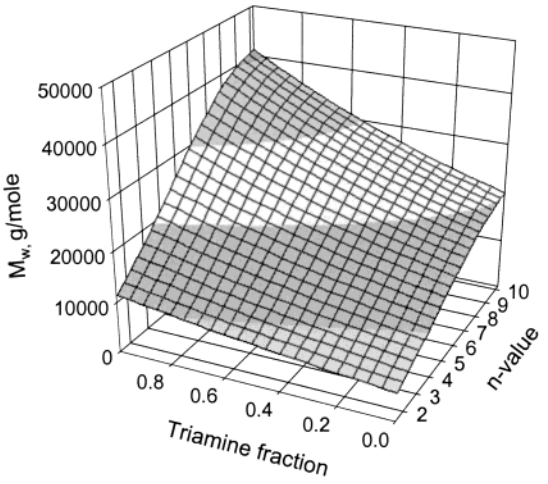

Figure 3. Graph of the response surface model of M_w versus triamine fraction and *n* value.

Because TGA was run under normal laboratory conditions (i.e., not in a dry room), some moisture pick-up did occur while preparing to run these analyses, especially for the salt-containing films. For this reason, the amount of residual NMP was always coupled with the amount of water absorbed from the atmosphere after unsealing the films. In all cases, however, the weight lost up to 200 °C by TGA ranged from 1 to 4%. TGA-FTIR detected the presence of NMP and water in the evolved gases in those samples prepared in NMP, making the total amount of both evolved gases together never more than 4%. None of the films made from THF retained any solvent as evidenced by TGA-FTIR—all weight loss (at the most 3%) was from postprocessing absorbed moisture.

Typical DSC traces for films with and without lithium salt are shown in Figure 4. The neat films typically have two reversible transitions, a glass transition temperature (T_g) between −60 and −45 °C and a transition (T_m)

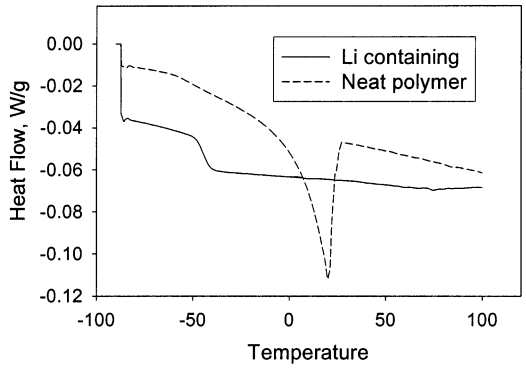

Figure 4. Typical DSC trace for films with and without lithium salt.

at approximately 18 to 25 °C, which is due to crystallization of the polyether coils as evidenced by wide-angle X-ray above and below this temperature.[11] This is consistent with DSC phase transitions reported for a similar polyalkyl ether polyimide block copolymer made from BTDA and an amine capped polyether alone (e.g., no aromatic diamine or triamine in the rod block) and proposed as switchable materials for electrochromic devices.[12]

In the lithium-salt-containing films, the T_g is somewhat more pronounced and higher than that of the neat films depending on salt concentration. The crystalline transition is completely suppressed in the salt-containing films for lithium-to-oxygen ratios of at least 0.05, and greatly reduced in size for the lower salt concentrations.

To discern any significant relationships between the variables and T_g, the values for T_g were analyzed by multiple linear least-squares regression. A mathemati-

(11) Eby, R. K., private communication. This is under further investigation and will be reported elsewhere.

(12) Michot, C.; Baril, D.; Armand, M. *Sol. Energy Mater. Sol. Cells* **1995**, *39*, 289−299.

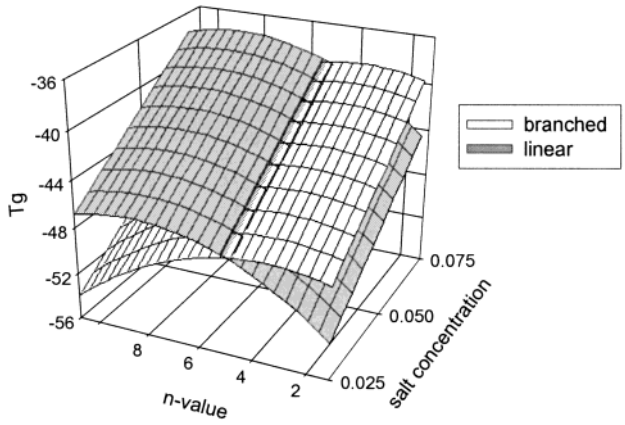

Figure 5. Response surface model of T_g vs. n value and salt concentration.

cal model describing the T_g in terms of the salt concentration, n value, percent triamine, and solvent was derived. All independent variables were again transformed to the −1 to 1 range prior to modeling to minimize correlation among terms. The previously described 14-term model was entertained, and terms not statistically significant (<90% confidence) were dropped from the model one at a time by the stepwise modeling technique.

A graph of the response surface model for T_g is shown in Figure 5. Significant terms in the model included first-order effects of salt concentration and triamine concentration, and a second-order effect of n value, with salt concentration being the most dominant. An interactive/synergistic effect of triamine concentration with n value was also significant. This interaction is clearly shown in Figure 5. When $t = 0$ (100% linear polymers), T_g increases with increasing n value (higher molecular weight). When $t = 1$ (100% branched polymers), T_g decreases with increasing n value. No terms containing solvent were significant in the model. Standard error of regression for the model was 1.05 °C with an $r^2 = 0.95$.

The values for T_m were also analyzed by multiple linear least-squares regression in terms of n value, percent triamine, and polymerization solvent. Salt concentration was not considered because T_m is suppressed in the salt-containing films. A graph of the response surface model for T_m is shown in Figure 6. Significant terms in the model included first-order effects of solvent, n, and triamine concentration, and interactive/synergistic effects of triamine concentration with n, triamine with solvent, and n with solvent. Essentially, with THF as the solvent, T_m decreases dramatically with increasing molecular weight especially for the branched polymers. With NMP as solvent, there is a smaller but still significant effect of triamine fraction and n on the T_c. Standard error of regression for the model was 1.13 °C with $r^2 = 0.91$.

Ionic conductivity measured by electrochemical impedance is shown in Figure 7 for a sampling of the films. The conductivity was measured from 0 to 80 °C for all of the films in the design. For the films with salt concentrations from 0.05 to 0.075 Li:O, a second-order linear regression plot fit the data quite well through the whole range. The films with salt concentration at 0.025 Li:O exhibited a slight drop in conductivity at ap-

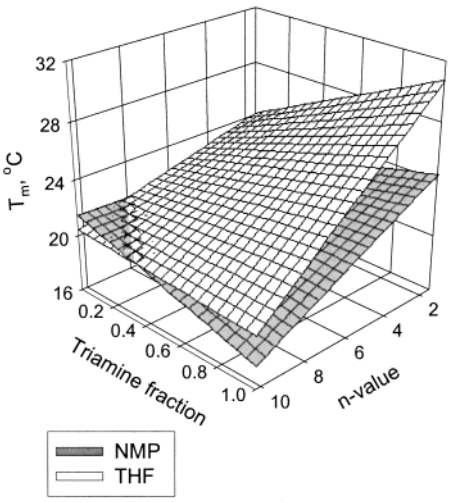

Figure 6. Graph of response surface model of T_m vs. triamine fraction and n.

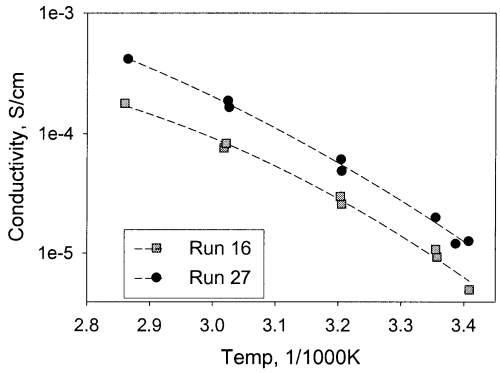

Figure 7. Plot of conductivity vs. temperature for selected experimental design runs.

proximately 20 °C, corresponding to the crystalline transition in the DSC. Because a second-order linear regression plot fits the data from 80 °C to just below room temperature ($r^2 > 0.98$) in all cases, ionic conductivity at 25 °C was interpolated for all the films from this fit.

The values for room-temperature (25 °C) ionic conductivity were analyzed by multiple linear least-squares regression as previously described for T_g. The conductivities were log-transformed for analysis. Significant terms in the model for ionic conductivity included first- and second-order effects of triamine concentration and salt concentration, and a second-order effect of n value, as well as an interactive/synergistic effect of triamine concentration with n value. Standard error of regression for the model was 0.081 with an $r^2 = 0.78$.

The response surface model can be used to predict the conditions that produce the optimum conductivity. In this case, conductivity is predicted to be at an optimum at 100% triamine concentration (fully branched) when the n value is at a maximum (10.72) and salt concentration is at 20:1 oxygen-to-lithium ratio. Under these conditions, room-temperature ionic conductivity is predicted to be 2.49×10^{-5} ***S***/cm (or log conductivity is −4.60). An actual film made with these conditions resulted in a conductivity of 2.45×10^{-5} *S*/cm (or log conductivity −4.61), which is in excellent agreement with the predicted optimum. Including this run in the

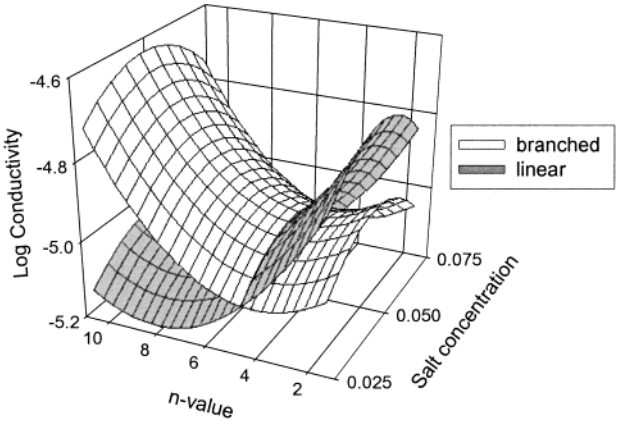

Figure 8. Plot of response surface model of ionic conductivity versus salt concentration and *n*.

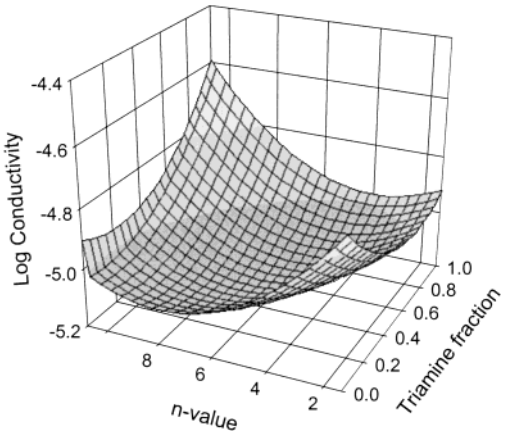

Figure 9. Plot of response surface model for ionic conductivity with salt at optimum ratio of 20:1 oxygen to lithium.

model reduces the standard error to 0.079 and increases r^2 to 0.83.

A predicted response surface model for log ionic conductivity vs salt concentration and *n*, and broken down into branched and linear polymers, is shown in Figure 8. From this figure, it is clear that the optimum salt concentration for any level of the other two variables is the mid-level of the design range. Also, this figure illustrates the strong interaction between number of repeat units, *n*, and triamine concentration, *t* (or extent of branching). The linear polymers ($t = 0$), shown as the shaded surface, decrease in conductivity with increasing *n*, while the branched polymers ($t = 1$) increase in conductivity with increasing *n*. This is probably due to the fact that the coils at the end of the polymers in the linear systems dominate the conductivity, and shorter polymers would have more chain ends per bulk. In the branched polymers, there is essentially a chain end in every repeat unit, offering no advantage to have a shorter chain.

The response surface with salt concentration held constant at the optimum value of 20:1 oxygen-to-lithium ratio is shown in Figure 9. This also shows the strong effect of increased branching (increased triamine concentration) especially in conjunction with increasing number of repeat units in the polymer.

No terms containing solvent were found to have a significant effect on ionic conductivity. It was thought that solvent could impact ionic conductivity because NMP has a much higher boiling point than THF. NMP

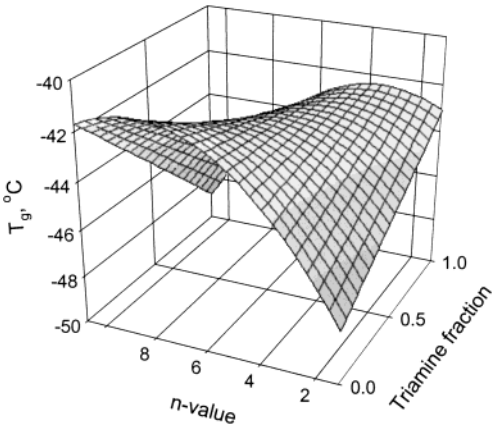

Figure 10. Plot of response surface model for T_g with salt at optimum ratio of 20:1 oxygen to lithium.

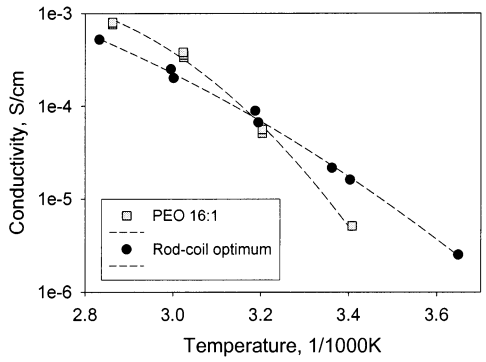

Figure 11. Ccomparison of ionic conductivity between the optimum rod−coil polymer formulation and state of the art PEO.

could therefore be present longer during processing in the oven and could also be more difficult to remove from the processed films. As previously discussed, there is very little residual solvent left even in the NMP-derived films. Dissolution of lithium salt in NMP was also a concern, as the salt dissolves in NMP alone only sluggishly. This proved, however, not to be a problem as salt readily dissolves in polyamic acid solutions in NMP or THF equally well.

A response surface of T_g with salt concentration held constant at the optimum value is graphed in Figure 10. When compared to Figure 9, this demonstrates a strong correlation of ionic conductivity on T_g.[13] The optimum values for ionic conductivity have the lowest T_g, and lowest conductive films have the highest values of T_g. Also like ionic conductivity, T_g appears to be dominated by the coils at the end of the polymers in the linear systems, giving rise to lower T_g for linear polymers of lower molecular weights. In the branched polymers, again the opposite trend is exhibited.

A plot of the log conductivity versus temperature of the optimum film is shown in Figure 11 compared with poly(ethylene oxide) containing the same lithium salt at its optimum ratio of 16:1 oxygen to lithium. The PEO film has slightly better conductivity at elevated temperatures, but falls off much more rapidly with decreasing temperature than the rod−coil polymer. At room

(13) The same correlation with T_g is observed for other polymers with ethylene oxide side chains. For example, see Lauter, U.; Meyer, W. H.; Wegner, G.; *Macromolecules* **1997**, *30*, 2092−2101.

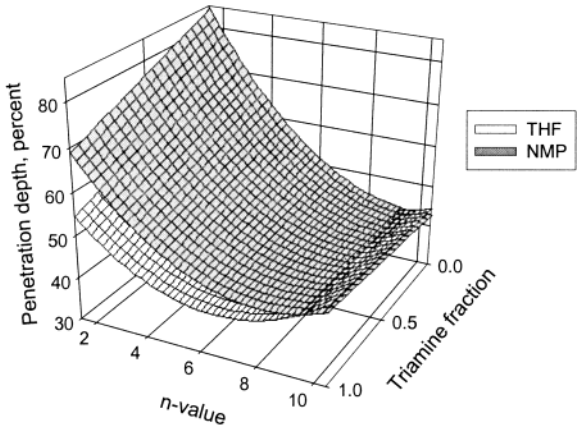

Figure 12. Plot of response surface model for percent penetration with salt at optimum ratio of 20:1 oxygen to lithium.

temperature, the rod−coil polymer has ionic conductivity of about an order of magnitude better than that of the PEO. At 0 °C, the rod coil polymer still has ionic conductivity comparable to that of the room-temperature PEO film.

Polymer films made from the optimum conditions for ionic conductivity were among the best in terms of physical properties as well. The highest molecular weight films, whether branched or linear, were robust, flexible, and quite elastic. Films at the other extreme were softer and tore easily. As a way of quantifying the physical properties of the films, a simple hardness test was done. A Shore Type-A hardness tester (BYK Gardener) was modified and applied to measure the depth of penetration for all the films.

Response surface modeling for percent penetration showed the most dominant effect to be *n* value as shown in Figure 12. Though minor, effects of triamine fraction and salt concentration were also evident. Triamine fraction was also present in the model as a two-way interaction with *n* value. At low *n*, percent penetration decreases with increasing triamine concentration, whereas at high *n*, there is almost no effect. Increasing salt concentration has the effect of softening the film and increasing penetration to a minor extent (approximately 5% across the whole range). This minor effect is not shown. Salt concentration (lithium-to-oxygen ratio) was held constant at 0.05 for the graph in Figure 12.

As shown in Figure 12, solvent is also significant in the model for percent penetration, but only as a two-way interaction with *n* value. The graph demonstrates this significant, synergistic effect of solvent with *n* value on the percent penetration. For lower *n* values, the percent penetration is predicted to be as much as 15% higher for the NMP runs, whereas at higher *n* values there is no difference in penetration between NMP and THF prepared films. Standard error of regression for the model was 5.4% with $r^2 = 0.86$. All terms in the model were greater than 91.5% significant.

Conclusions

This paper describes a series of rod−coil block copolymers that produce easy-to-fabricate, dimensionally stable films with good ionic conductivity down to room temperature for use as electrolytes for lithium polymer batteries. The polymers consist of short, rigid, rod polyimide segments alternating with flexible, polyalkylene oxide coil segments.

An optimization study was carried out to study the effects of four variables (degree of branching, formulated molecular weight, polymerization solvent, and lithium salt concentration) on ionic conductivity, glass transition temperature, and dimensional stability in this system. The results of the experimental design show that highest molecular weight polymers studied with the largest degree of branching have the best conductivity. Optimum salt concentration for the films to produce the best conductivity was at a ratio of 20:1 polyether oxygens to lithium ions. The polymerization solvent had no effect on either the conductivity or the glass transition temperatures of these polymers, most likely because the amount of residual solvent after processing was small for all the films. Fortuitously, polymer formulations giving the best ionic conductivity also were among the most robust, flexible, and elastic films. Because the optimum formulation was at the upper limits of the design, it may be possible to raise the ionic conductivity even more in these systems by exploring ways to increase the degree of branching further with the use of smaller rod repeat units or shorter coil side chains.

Acknowledgment. We thank Sarah H. Zaman for running the FT-IR analysis of the polymer films. We thank the Polymer Rechargeable Energy Systems Program (PERS) of NASA Glenn Research Center for support of this work.

CM0301726